Soil water and carbon dynamics of barley - pea intercropping in a temperate environment under projected climate change

Oludare S. Durodola [a,b,*] , Cathy Hawes [b] , Jo Smith [c] , Tracy A. Valentine [b] , Josie Geris [a]

[a] School of Geosciences, University of Aberdeen, AB24 3UF, Aberdeen, UK
[b] Ecological Sciences Department, The James Hutton Institute, DD2 5DA, Dundee, UK
[c] School of Biological Sciences, University of Aberdeen, AB24 3UU, Aberdeen, UK

HIGHLIGHTS

- Water-carbon dynamics are predicted for temperate intercropping vs monoculture.
- Intercropping showed similar evapo-transpiration to monoculture over the long-term.
- Intercropping increased plant transpiration but had less variability in water use in dry years.
- Intercropping is projected to increase soil carbon by 16 % over monoculture by 2050.

GRAPHICAL ABSTRACT
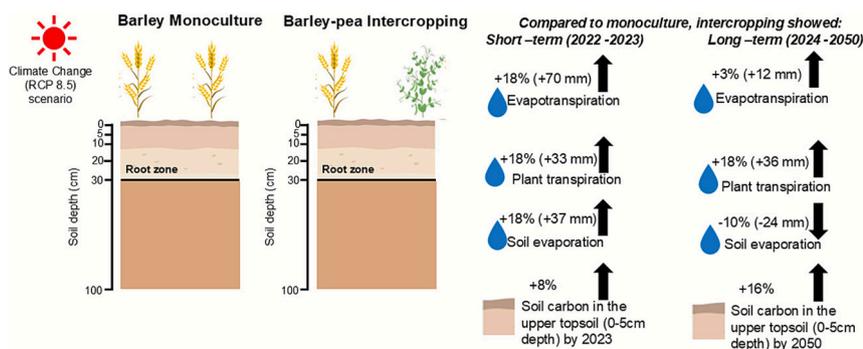
ARTICLE INFO

ABSTRACT

Intercropping is an emerging potential nature-based solution for sustainable crop production in temperate environments. However, its long-term role in contributing to climate mitigation and adaptation remains unclear. This work presents the first evidence of potential long-term water and carbon effects of barley (*Hordeum vulgare* L.) and pea (*Pisum sativum* L.) intercropping versus its barley monoculture for a typical temperate environment in Scotland. Based on experimental data, water (HYDRUS 5) and soil carbon (RothC) models were coupled to project water-carbon dynamics for the short-term during a two-season field trial (2022–2023) and the long-term future (2024–2050) under a worst-case climate scenario (Representative Concentration Pathway, RCP 8.5). The coupled water-carbon model effectively captured the water-carbon dynamics observed in the short-term. Compared to barley monoculture, intercropping increased evapotranspiration up to ~20 % in the short-term, dominated by the dry weather conditions in 2022. Long-term intercropping projected lower interannual variability in evapotranspiration than barley monoculture, but showed higher plant transpiration in dry years, indicating more adaptive water use and hydrological resilience. As intercropping is projected to increase transpiration but reduce soil evaporation compared with barley monoculture, it maintained similar levels of soil water content and storage in the topsoil (0–30 cm). In addition, by 2050, soil carbon was predicted to increase in

the upper topsoil (0–5 cm) of intercropping by 16 % (1.91 kg m^{-2}) compared to barley monoculture (1.63 kg m^{-2}). These novel findings suggest that intercropping could play a critical role in enhancing hydrological resilience and carbon sequestration in temperate environments for sustainable land management.

1. Introduction

Climate change is intensifying pressure on land resources globally by elevating temperatures and shifting precipitation patterns causing soil degradation, low agricultural productivity and food insecurity (IPCC, 2023). In humid temperate climates, where water has not previously been limiting for plant growth, periods of water scarcity are increasingly occurring and projected to intensify in the future (IPCC, 2023; Visser-Quinn et al., 2021). Drought frequency in Scotland is projected to double by 2050, with significant challenges to major sectors, including the agricultural, food and drink industries (Glendell et al., 2024; Visser-Quinn et al., 2021). This relates directly to shifts in precipitation patterns and temperature extremes leading to elevated evapotranspiration, decreased soil water storage, and increased water stress (Glendell et al., 2024).

Soil carbon (C) is a factor that is key in achieving both climate change adaptation and mitigation (Li et al., 2024). Nature-based solutions, such as those included in agroecological or regenerative practices, provide the potential to enhance C storage in soils (Begum et al., 2022; Prudil et al., 2023), and present economic opportunities for farmers to access C credit markets (Raina et al., 2024). Furthermore, soil C is integral to overall soil health, including its water holding capacity (Rodriguez et al., 2020; Yu et al., 2022). This underpins the long-term productivity and resilience of agroecosystems (Smith et al., 1997). While experimental evidence has been collected for these benefits at relatively short timescales (Begum et al., 2022; Li et al., 2024), the long-term sustainability potential for C sequestration remains unclear; this highlights the need for modelling approaches.

One promising nature-based solution in arable agriculture, gaining attention in temperate environments, is intercropping. This involves two or more crop species or varieties being grown simultaneously in the same field, deployed in mixed, row, strip or relay patterns (Durodola et al., 2025; Stomph et al., 2020). Monoculture systems typically rely on the intensive use of agrochemical inputs, including synthetic fertilisers, pesticides and herbicides (Stomph et al., 2020), while intercropping practices provide potential for maintaining crop yield and productivity with reduced inputs (Rodriguez et al., 2020).

In temperate environments, cereal - legume combinations are of particular interest due to their adaptability to climatic and soil conditions, while legumes also enhance nitrogen use efficiency and reduce reliance on synthetic fertiliser inputs for cereals (Rodriguez et al., 2020). Additional beneficial effects of intercropping in temperate environments have been reported to include increased yields and land productivity (Brooker et al., 2024), higher N fixation (Rodriguez et al., 2020) and enhanced water uptake during periods of water stress (Durodola et al., 2025).

However, previous studies have mainly focused on the short-term (≤3 years) benefits of intercropping, while the potential long-term effects remain unknown. Global syntheses have shown that in the short-term, diverse intercropping systems can reduce runoff by 13 - 45 % and soil evaporation by 3 - 18 %, while increasing plant transpiration by 20 - 40 % and water use efficiency by 6 - 45 %, resulting in similar soil volumetric water content (VWC) compared with monocultures (Liu et al., 2025; Yin et al., 2020). For example, Fan et al. (2016) found that maize - potato intercropping reduced evaporation and runoff, while it increased transpiration and soil VWC compared to maize and potato monocultures in China. Maize - soybean intercropping also showed similar evapotranspiration with monocultures, but reduced soil VWC and soil evaporation during a 2-year experiment, with effects dependent on the sowing ratio/pattern (Rahman et al., 2017).

In another global synthesis (Li et al., 2024), it was found that intercropping increased soil C by 8 - 18 % compared to monocultures, with the top 0–20 cm soil depth showing the most accumulation. For example, during a 7-year field experiment in China, intercropping-rotation of maize-wheat, maize-faba bean and wheat-faba bean systems increased soil C by 4 % in the top 20 cm of soil (Cong et al., 2015). Potato - soybean intercropping also increased soil C by 7.8 % compared to monoculture during a 7-year field experiment (Wang et al., 2025a). These outcomes were mainly influenced by crop/cultivar combination and soil depth. However, these studies are predominantly from non-temperate environments and were carried out over short- to medium-term (≤ 7 years) timescales, highlighting the gap this study aims to fill.

Since most of the existing evidence originates from non-temperate environments, where climatic conditions, soil types and crop species differ substantially from those in temperate environments, their relevance to temperate environments remains unclear. There is, therefore, limited understanding of the long-term (≥25 years) resilience and rate of soil C sequestration in intercropping under future climate scenarios, especially in temperate environments. Understanding how intercropping systems could affect soil moisture and C sequestration in temperate environments under projected climate change is essential for the wider adoption of intercropping as a potential climate-resilient practice and to inform policy (Durodola et al., 2025). While some experimental and modelling studies have explored the short-term benefits of intercropping, most have not considered how these systems would perform over the long term in response to projected climatic changes.

Coupled water and C modelling, especially when based on empirical data, provides a viable approach to understanding the potential long-term and future effects of intercropping on water and C dynamics. Process-based models such as HYDRUS (for simulating soil water dynamics) and RothC (for C turnover and sequestration) in intercropping could therefore provide important insights into its potential for climate change adaption, and sustainable land and water management (Begum et al., 2022; Šimůnek et al., 2024; Wang et al., 2024a).

The aim of this study is, therefore, to examine the long-term effects of temperate intercropping on water and C dynamics under a worst-case climate scenario. The Representative Concentration Pathway 8.5 (RCP 8.5) (Reyniers et al., 2025) was selected as a high-emission climate scenario to assess the potential resilience of intercropping under extreme and adverse future conditions. More specifically, the objectives were to:

1. Calibrate and evaluate a coupled water and C modelling approach to simulate short-term (two years) observed soil water and C dynamics of barley-pea intercropping and barley monoculture.
2. Extrapolate simulations to provide long-term future (2024–2050) water and C dynamics of intercropping and barley monoculture under a worst-case climate change scenario (RCP 8.5) using the same approach.
3. Explore the effects of barley-pea intercropping as opposed to barley monoculture on water availability and C storage in the long-term.

This study focused on the intercropping of spring barley (*Hordeum vulgare* L.) and pea (*Pisum sativum* L.) in North-East Scotland, UK. Barley was selected for its economic relevance to the UK food and drink sectors, and pea was chosen as a nitrogen-fixing legume commonly used in animal feed. This study is based on short-term empirical data collected during the experimental period from 2022 to 2023 (Durodola et al., 2025, 2026), providing the foundation for calibrating and evaluating the soil water and C modelling approach. The modelling approach followed

the coupling of HYDRUS (Version 5) with the RothC model for soil water and C dynamics, respectively. To our knowledge, this study represents the first attempt to model the long-term effects of intercropping on soil water and C dynamics under future climate conditions.

2. Materials and methods

2.1. Study site and experimental design

Experimental data were collected at Balruddery Farm, a research facility of the James Hutton Institute, near Dundee in North-East Scotland, UK (56.48°N, 3.11°W; 67-163 m above sea level) (Fig. S1). The site is within a temperate climate zone, characterised by a long-term average annual precipitation and a mean daily temperature of 800 mm and 8.6 °C, respectively (Hawes et al., 2018). The soil at the farm is Cambisol according to the World Reference Base for Soil Resources, with a sandy loam and clay loam texture and topsoil depth of 30 cm (Hawes et al., 2018). The field used for this study, known as *Grieves House,* has sandy loam texture within the topsoil (41.74 % sand, 46.55 % silt and 11.71 % clay), bulk density of 1.33 g cm^{-3} and pH of 6.2.

Field trials were conducted over two consecutive years (18 April - 16 September 2022 and 27 March - 25 August 2023) across 20 (6.25 m × 1.5 m) experimental plots to evaluate barley - pea intercropping systems in comparison to their respective monocultures. The experiment included four cropping systems, each with five replicates, arranged in a randomised complete block design (Fig. S2). Treatments comprised two monocultures and two barley–pea intercropping systems involving two barley cultivars (Laureate and KWS Sassy) and one pea cultivar (LG Stallion) as described in Durodola et al. (2025, 2026). Intercropping systems were established using a mixed-replacement design with sowing density of 70 % barley and 30 % pea. In a replacement design, a proportion of one crop species is substituted by another, while maintaining the total sowing density equivalent to that of the corresponding monocultures. The experiment followed low-input management, with no agrochemical applications during the growing seasons. Prior to the study, the plots were under barley monoculture for several years but changed to cover cropping (a mix of rye, vetch, triticale, fodder radish, brown mustard, buckwheat, and clover) and no-tillage management three years before the experiment. Plots were inversion ploughed to 20 cm deep prior to seed drilling. A full description of the field layout and field management is reported in Durodola et al. (2025, 2026). In this study, the focus is on the barley (Laureate) - pea intercropping and its barley monoculture, where increases in soil C for the intercropping system were observed during the experiment (Durodola et al., 2026). This study could not consider pea monoculture since empirical data on plant water uptake were only available for barley monoculture during the experimental period, constraining the ability to simulate pea monoculture.

2.2. Data collection

2.2.1. Short-term meteorological and soil water measurements

Daily weather data and soil VWC (Fig. 1) covering the study period were obtained from the COSMOS-UK Met Station (56.482°N, 3.112°W; elevation 130 m; https://cosmos.ceh.ac.uk/), situated about 320 m south of the study site (Fig. S1). The data (hereafter referred to as the COSMOS data) provided high temporal resolution measurements via cosmic ray neutron sensing (Smith et al., 2024). In addition, historical daily climatic records (1960 - 2021) were sourced from the UK Met Office Mylnefield Station (56.456°N, 3.069°W; elevation 26 m), which covers the catchment and is situated about 5.1 km southeast of the study site.
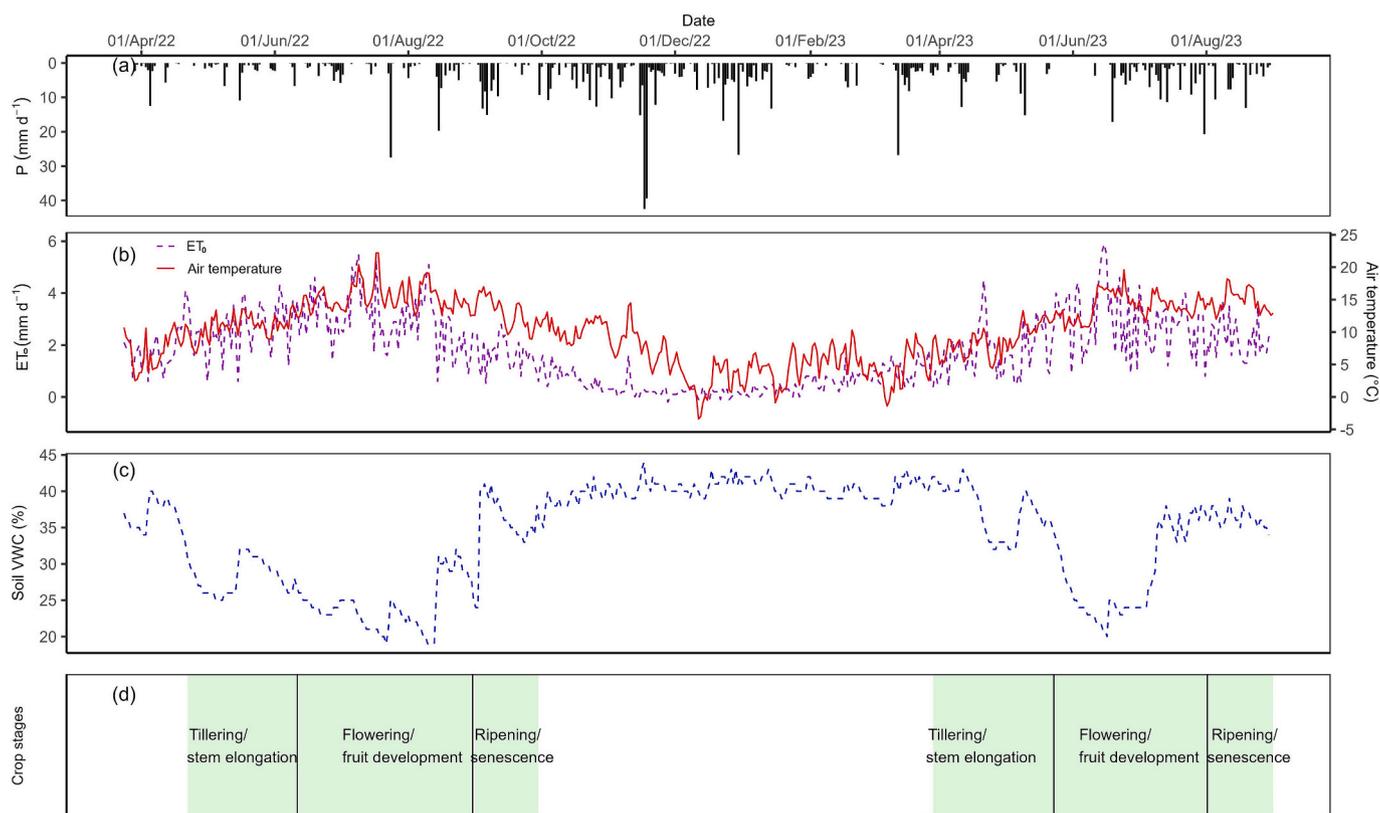

Fig. 1. Hydro-climatological data during the short-term study period. (a) Daily Precipitation amount (P, mm d^{-1}); (b) air temperature and potential evapotranspiration (ET_0) estimated with weather station data and the Penman-Monteith equation; (c) daily soil volumetric water content (VWC) for the upper ~15 cm soil depth measured at the COSMOS Met Station (https://cosmos.ceh.ac.uk/); (d) phenological crop growth stages. The green bands represent the periods of each growth stage.

The first experimental year (October 2021 - September 2022) was drier and warmer compared to the second year (October 2022 - September 2023) (Fig. 1). Both years followed similar seasonal trends, with mean daily air temperatures rising from approximately 5 °C in April to over 20 °C in summer, then gradually decreasing by late August (Fig. 1). Daily potential evapotranspiration (ET_0), as estimated from the weather station climatological data using the Penman-Monteith equation (Allen et al., 1998), followed the same pattern.

In 2022, in-situ VWC was measured during the growing season at 5 cm depth on 11 and 24 May; 15 and 29 Jun; and 05 and 19 August using SM300 time domain reflectometry (TDR) sensors (Delta-T Devices Ltd., Cambridge, UK) across 8 sampling points ($n = 8$) in each plot. In 2023, TDR measurements were taken at 5 cm and 10 cm depths on 16 May, 22 June and 18 July.

Daily timeseries of in-situ soil VWC (hereafter referred to as in-situ probes data) were obtained at the experimental plots in 2023 (not measured in 2022), as reported in Durodola et al. (2025). The in-situ probes data were measured from April to August at 10, 20, 30, and 40 cm depths in one replicate of the four cropping systems ($n = 4$) using PR2 SDI-12 Soil Moisture Profile Probes (Delta-T Devices Ltd., Cambridge, UK). A relationship between 2023 TDR and in-situ data was established and subsequently applied to adjust the 2022 TDR values (hereafter referred to as 2022 TDR-corrected data), thereby minimising methodological discrepancies. However, due to small-scale spatial heterogeneity in soil properties, clear distinctions in VWC among the cropping systems were not discernible in either 2022 or 2023 (Durodola et al., 2025). Therefore, for the HYDRUS soil profile modelling setup (Section 2.3), a representative profile from the four replicates at each depth were used similarly for both intercropping and monoculture systems.

2.2.2. Short-term plant root water uptake

Data on barley root water uptake depths during the field experiment in both intercropping and monoculture systems were previously reported in Durodola et al. (2025). Those data quantified the proportional contributions of different soil water sources (upper topsoil, < 5 cm and lower topsoil, 5-30 cm depths) to barley water uptake. To estimate the proportional water uptake contributions, water stable isotopes (δ^2H and $\delta^{18}O$) were used to explore water uptake patterns during different hydro-climatological conditions, offering insights into niche differences in water uptake between barley in intercropping and monoculture (Durodola et al., 2025). To support this, isotope sampling was conducted on 19 Aug 2022, 16 May 2023, 22 June 2023 and 18 July 2023 across key crop growth stages, covering 2022 and 2023. The HYDRUS modelling was based on plant water uptake data, providing a qualitative assessment of the model's ability to capture soil water uptake dynamics under both intercropping and monoculture systems.

2.2.3. Short-term soil carbon data

Historical soil C stock and bulk density data measured at the study site five years prior to the study were obtained from the Farm records while the data measured during the field experiment in both intercropping and monoculture systems are reported in Durodola et al. (2026) (Table S1). The historical data were obtained for the upper topsoil (<5 cm depth) at post-harvest in September each year, while reported data in Durodola et al. (2026) were also collected from the same depth at pre-sowing in March and post-harvest in September each year.

2.2.4. Long-term climate change scenario data

To assess the potential long-term future impacts of climate change, the bias-corrected projections for precipitation (P), air temperature (T) and potential evapotranspiration (ET_0) of the study site up till 2050 based on the high greenhouse gas emissions RCP 8.5 scenario were employed. Opting for a worst-case scenario allows us to capture the full range of potential climate risks and test whether intercropping as a

mitigation strategy is viable even in the most adverse of plausible conditions. While RCP8.5 may represent a less likely future under current mitigation policies, it is useful for identifying management strategies that are robust across a wide range of climate outcomes and could therefore support robust decision making. The projections were provided by Reyniers et al. (2025) and were derived from the UK Climate Projections 2018 (UKCP18) using the downscaled Regional Climate Model output from the 12 km resolution Perturbed Physics Ensemble (UKCP18-RCM-PPE) across 12 ensemble members. They estimated ET_0 using the Penman–Monteith method (Allen et al., 1998), after which all the datasets were bias-corrected using a variant method of quantile mapping developed for the third phase of the Inter-Sectoral Impact Model Intercomparison Project (ISIMIP) (Reyniers et al., 2022a, 2022b). The biases in the dataset for the study site were corrected by multiplying the P, T and ET_0 timeseries obtained from Reyniers et al. (2022a, 2022b, 2025) by correction factors (Ehret et al., 2012). These correction factors were estimated as 0.81, 1.03, and 1.16, for P, T and ET_0, respectively. The factors were estimated by the average of UK Met Office observed values between 1960 and 2021, divided by the average projected data for the same timeframe.

Compared to the 1960 - 2021 long-term average, P is projected to decrease by 5 % during April - September while it is projected to increase by 35 % during October - March, though changes are expected to be highly variable between extreme wet and dry years (Table S2). Also, T is projected to increase by 10 % in all months, steadily rising from average annual of 12.7 °C in 2024 to 13.1 °C by 2050, while annual ET_0 is projected to increase from an average of 2.2 to 2.9 mm day^{-1} in warm years. Overall, climate extremes (hotter and drier summers, as well as wetter autumn and winter seasons) are expected to become more frequent from the 2040s onwards.

2.2.5. Standardised precipitation and evapotranspiration index

The 3-month Standardised Precipitation and Evapotranspiration Index (SPEI) was used to categorise all study years (2022 - 2050) into hydro-climatological conditions relevant for agricultural water availability: dry, normal, and wet. SPEI was selected for incorporating both precipitation and temperature anomalies, reflecting the combined effects of drought and elevated temperatures expected under future climate scenarios, while a 3-month timescale reliably captures short- and medium-term soil water variability critical for crop growth and useful for agricultural forecasting (Vicente-Serrano et al., 2010). Years with SPEI value(s) below -1.5 were classified as dry, values above 1.5 as wet, and those between as normal. Accordingly, the years 2022, 2025, 2036, 2044, and 2047-49 were identified as dry; 2024, 2028, 2033, 2042 and 2045 as wet, and all other years as normal (Fig. S3).

2.3. HYDRUS 2-D model configuration

2.3.1. Description of HYDRUS model and modelling parameters

The HYDRUS 5 (2D) software (Šimůnek et al., 2024; Šimůnek and van Genuchten, 1999) was used to simulate soil water dynamics due to its ability to resolve unsaturated flow with high vertical accuracy (<1 mm) by solving the Richards equation and accounting for detailed soil hydraulic properties via the van Genuchten (1980) model.

Water flow in isotropic unsaturated soil was numerically solved in the model using a modified Richards' equation, Eq. (1) (Šimůnek et al., 2016, 2024).

$$\frac{\partial \theta}{\partial t} = \frac{\partial}{\partial x}\left[K(h)\frac{\partial h}{\partial x}\right] + \frac{\partial}{\partial z}\left[K(h)\left(\frac{\partial h}{\partial z}+1\right)\right] - S(h,h_\varphi)\frac{\partial \theta}{\partial t}$$
$$= \frac{\partial}{\partial x}\left[K(h)\frac{\partial h}{\partial x}\right] + \frac{\partial}{\partial z}\left[K(h)\left(\frac{\partial h}{\partial z}+1\right)\right] - S(h,h_\varphi) \tag{1}$$

where θ is the soil VWC (cm^3 cm^{-3}), h is the pressure head (cm), h_φ is the osmotic head (cm), $K(h)$ is the hydraulic conductivity function (cm day^{-1}), t is time (day), S is the root water uptake (cm^3 cm^{-3} day^{-1}), x is

the horizontal coordinate (cm), and z is the vertical coordinate (cm) (note that all parameters are listed and defined in Table S3).

Root water uptake (S) under water stress conditions is described in Eq. (2) (Feddes et al., 1978). HYDRUS code was modified to consider water uptake of two different vegetations, i.e., to allow different parameters for root water uptake by barley and pea following Chen et al. (2020, 2022a), Eq. (3).

$$S(h) = \propto(h)b(x,z,t)T_pL_p \tag{2}$$

$$S(h) = S_1(h) + S_2(h) = \propto_1(h)b_1(z)T_{p1} + \propto_2(h)b_2(z)T_{p2} \tag{3}$$

where $\propto$ is the stress response function (unitless), b represents the spatial distribution of roots in the rootzone (cm^{-1}), and T_p is the potential transpiration (cm day^{-1}), subscripts 1 and 2 refer to barley and pea, respectively, L_p is the length of the soil surface associated with transpiration (cm), L_p values of 50 cm in barley monoculture and barley – pea intercropping were used, and $b(x,z,t)$ is the normalized root water uptake distribution function (cm^{-2}).

HYDRUS requires potential evapotranspiration separately as potential evaporation (E_p) and transpiration (T_p), describing the potential rate of root water uptake and evaporation from the soil surface under sufficient water availability, respectively. First, potential crop evapotranspiration (ET_p) was obtained by multiplying ET_0 with the crop coefficient (K_c), Eqs. (4)–(5), determined using the single crop coefficient approach (Allen et al., 1998).

$$ET_p = K_c \times ET_0 \tag{4}$$

$$ET_p = T_p + E_p \tag{5}$$

where ET_p is potential crop evapotranspiration (cm day^{-1}), T_p is the potential transpiration rate (cm day^{-1}), ET_0 is the potential evapotranspiration (cm day^{-1}), and K_c is crop coefficient (unitless). The required daily weather data (E_p, T_p and ET_0) used in the above calculations for 2022-2023 were obtained from the COSMOS weather station while for 2024–2050, they were obtained from the future climate dataset.

For the intercropping, K_c was estimated using a comprehensive coefficient without considering the height difference between the two crops (Allen et al., 1998; Wang et al., 2024a), Eq. (6).

$$K_c = \frac{P_b K_{c,b} + P_p K_{c,p}}{P_b + P_p} \tag{6}$$

where P_b and P_p are sowing area proportions of barley ($P_b = 0.7$) and pea ($P_p = 0.3$) in the intercropping system, and $K_{c,b}$ and $K_{c,p}$ are the crop coefficients of barley and pea, respectively, as obtained from Allen et al. (1998). $K_{c,b}$ is 0.30, 1.15 and 0.25 while $K_{c,p}$ is 0.50, 1.15 and 1.10 during the early season, mid- season, and late season, respectively (Table S4).

E_p is estimated as Eq. (7) (Belmans et al., 1983)

$$E_p = ET_p \ e^{-k.LAI} \tag{7}$$

where k is the radiation extinction coefficient, which is 0.46 for barley (Geris et al., 2021) and 0.53 for pea (Robertson et al., 2001), and LAI refers to the leaf area index (no units).

Daily LAI of spring barley monoculture was obtained from Baruth et al. (2012) as monitored in East Anglia, UK. The LAI of spring pea monoculture (unpublished) was obtained from Processors and Growers Research Organisation (PGRO), as monitored in Peterborough, UK in 2023. T_p for barley and pea in the intercropping system was estimated as 70 % of the T_p of barley monoculture and 30 % of the T_p of pea monoculture, respectively, based on the mix ratio.

The root density distribution was configured using the Vrugt model with a maximum rooting depth of 80 cm, maximum root intensity set at 5 cm (10 cm for intercropping), and a shape parameter of 1, using Feddes

model root water uptake parameters in HYDRUS. Feddes model root water uptake parameters were not available for barley at the study site, so Feddes wheat and pea parameters were used instead (Feddes et al., 1978). The root distribution of barley was subsequently adjusted based on the barley root water uptake data reported in Durodola et al. (2025) which indicated that the upper topsoil (< 5 cm) water is the dominant source for barley monoculture during different crop growth stages, with deeper water acquisition from lower topsoil (5-30 cm) depth under intercropping. Barley root distribution was set for monoculture as 0.6, 0.2, 0.1, 0.1 and for intercropping as 0.4, 0.3, 0.2, 0.1 at 0 - 5, 5 - 10, 10 - 20, 20 - 30 cm depths, respectively. The root distribution of intercropped pea was not adjusted, as no measurements were available.

Change in seasonal (Apr - Aug) soil water storage for each year was determined by Eq. (8).

$$\Delta S = P - ET_a - D \tag{8}$$

where ΔS is the water storage change in the soil rooting zone (i.e. upper 30 cm), D is the deep percolation leaving the 30 cm depth and ET_a is simulated actual evapotranspiration. Lateral fluxes were neglected due to no-flux boundaries.

2.3.2. Modelling conditions, calibration and validation

Soil water dynamics were simulated within a 100 cm $\times$ 50 cm rectangular domain (Fig. S4). Boundary conditions included an atmospheric boundary at the top, free drainage at the bottom (reflecting the freely draining nature of the soil), and no-flux boundaries along the left and right boundaries. Soil layers were defined as 0 - 10, 10 - 20, 20 - 30, and 40 - 100 cm.

The model was calibrated with the 2023 in-situ probes VWC data for both intercropping and monoculture systems due to its higher temporal and spatial coverage, providing a robust setup. For calibration, the model was initially set up using the in-situ probes VWC data as the initial conditions on 12 April 2023 set to 18, 23, 26, 24, and 39 % at 10, 20, 30, 40, and 40–100 cm depths, respectively. Bulk density and soil texture data were inputted to the Rosetta pedotransfer functions to estimate soil hydraulic parameters for each soil layer with the van Genuchten-Mualem model using the neural network approach (Schaap et al., 2001). The hydraulic parameters were residual VWC (θ_r, %), saturated VWC (θ_s, %), inverse air-entry suction (α, cm^{-1}), pore size distribution index (n, unitless), saturated hydraulic conductivity (K_s, cm day^{-1}) and pore connectivity parameter (l, unitless). These parameters were then optimised using a Marquart-Levenberg-type parameter optimisation module (Lazarovitch et al., 2009) to ensure a fit between simulated and observed VWC. The 2022 TDR-corrected VWC data was then used for validating the fit between simulated and observed VWC.

HYDRUS performance in simulating the short-term soil water dynamics was evaluated using the coefficient of determination (R^2), root mean square error ($RMSE$), and the Kling–Gupta Efficiency (KGE). R^2 estimates the proportion of variance explained by a model, where values closer to 1 indicate stronger agreement between observed and simulated values. $RMSE$ quantifies the average magnitude of prediction errors (in same units as the measurements), lower values indicate optimal model performance, Eq. (9). It was also expressed as a percentage by multiplying by $\frac{100}{\mu_o}$ (where μ_o is the average of the observed values). KGE is a composite metric that combines correlation, bias and variability, with values closer to 1 indicating optimal model performance (Gupta et al., 2009), Eq. (10). KGE values greater than -0.41 indicates model is better than using mean observation, but only values between 0.4 and 0.6 are deemed 'acceptable' and above 0.6 generally are deemed as 'good'.

$$RMSE = \sqrt{\frac{\sum_{i=1}^{n}(O_i - S_i)^2}{n}} \tag{9}$$

$$KGE = 1 - \sqrt{(r-1)^2 + \left(\frac{\sigma_s}{\sigma_o} - 1\right)^2 + \left(\frac{\mu_s}{\mu_o} - 1\right)^2} \qquad (10)$$

where r is the linear correlation coefficient between the simulated (S_i) and observed (O_i) values, n is number of observations, σ_s and σ_o are the standard deviations in the simulations and observations, respectively, and μ_s and μ_o are the mean of the simulations and observations, respectively.

Since the short-term observed VWC was comparable between intercropping and barley monoculture, a qualitative approach was adopted to assess the model's performance in capturing system-specific dynamics. Model evaluation focused on the proportional distribution of barley water uptake across different soil depths, providing insight into the spatial patterns of root water uptake (Durodola et al., 2025). This allowed confirmation that the model accurately represented water uptake dynamics characteristic of both intercropping and monoculture.

To capture the full seasonal dynamics following soil hydraulic calibration, HYDRUS was simulated for the short-term (2022−2023), following a spin-up of 3 years with optimal soil water conditions as initial conditions. For the long-term future (2024–2050), simulations were run continuously with 1 April and 31 August as sowing and harvesting dates, respectively, representing a typical spring growing season. To isolate the effects of climate variability on water use, management practices were held constant across years, with weather data being the only variable input.

The results of soil water dynamics are presented for the top 30 cm of the soil profile in this study, since that is where the roots and water uptake are concentrated in this type of environment (Durodola et al., 2025).

2.4. Rothamsted carbon model (RothC) configuration

2.4.1. Description of RothC

The Rothamsted C model (RothC; (Coleman and Jenkinson, 2024, 1996)) simulates soil C dynamics through four active soil organic matter pools; decomposable plant material (DPM), resistant plant material (RPM), humified soil organic material (HUM) and soil microbial biomass (BIO), and an inert organic matter pool (IOM). RothC partitions incoming plant residues into RPM and DPM based on the DPM:RPM ratio defined according to land use type. The plant material decomposes to form CO_2, BIO and HUM, with all active pools undergoing decomposition by first-order processes, each with different decomposition rates. Decomposition rates are modified monthly based on the soil VWC, temperature, pH and plant cover, according to the conditions of that month (Falloon et al., 1998). Soil clay content (texture) affects the partitioning of decomposing organic matter into CO_2, BIO and HUM.

The IOM pool, C_{IOM} (kg m^{-2}), was estimated from the observed total C using the Falloon equation, Eq. (11), (Falloon et al., 1998).

$$C_{IOM} = 0.049 \times C_o^{1.139} \qquad (11)$$

where C_o is the observed C (kg m^{-2}).

RothC operates in two modes, a forward mode, which uses known C inputs to simulate C changes, and an inverse mode, used to estimate C inputs and initial pool sizes based on observed soil C at steady state (Smith et al., 2007). Monthly C dynamics in each pool are computed as Eq. (12) (Coleman and Jenkinson, 2024, 1996):

$$C_{end} = C_{start} \times e^{-abwcdk_r/12} \qquad (12)$$

where a, b_w and c are rate modifiers for temperature, soil water and soil cover, respectively (Coleman and Jenkinson, 2024); d is the rate modifier for soil pH; k_r is the decomposition rate constant 10.0 y^{-1} (DPM), 0.3 y^{-1} (RPM), 0.66 y^{-1} (BIO), and 0.02 y^{-1} (HUM) (Coleman and Jenkinson, 2024); C_{end} is C in the pool at the end of the month, C_{start} is C in the pool at the beginning of a month, both in kg m^{-2} (or t ha^{-1}), and 12 is a

constant converting the yearly rate constant to a monthly value. The sum of these pools gives the total active C.

2.4.2. Interpolation procedure of RothC model

Weather (current and future scenarios), plant and soil data obtained were entered into RothC (Table S1). The DPM/RPM ratio was set to the default value of 1.44 for arable (i.e. 59 % of the plant material is DPM and 41 % is RPM) (Coleman and Jenkinson, 2024, 1996). The model was first run in inverse mode (to steady-state) to estimate monthly C inputs from plant residues, based on observed total C, clay content, IOM, climate and soil cover conditions (Smith et al., 2007). This steady-state run used weather data obtained from the UK Met Office and was continued until total soil C in two consecutive iterations differed by less than 0.0001 kg m^{-2} (steady-state) and matched the soil C measured in September 2022 (Table S1); this served as a baseline to assess the effects of future climate and management changes on soil C.

Because no long-term data are available for this intercropping system, RothC was then run in forward mode, iteratively adjusting C inputs for each crop in the rotation until the simulated C matched measured values. Note that the simulations were restricted to the 0 - 5 cm depth, where the obtained measurements showed significant difference between intercropping and barley monoculture systems (Durodola et al., 2026).

The fit of the adjusted RothC simulations to the measurements was quantified using R^2, $RMSE$ and KGE as described in Section 2.3.2. The statistical significance of $RMSE$ was also assessed by estimating its 95 % confidence threshold ($RMSE_{95\%}$, %) following (Smith et al., 1997), Eq. (13), using the standard error of observations.

$$RMSE_{95\%} = \frac{100}{\mu_o} \sqrt{\frac{\sum_{i=1}\left(t_{(n-2)95\%} \times S_e(i)\right)^2}{n}} \qquad (13)$$

where $t_{(n-2)95\%}$ is Student's t distribution with $n - 2$ degrees of freedom and a two-tailed P-value of 0.05, μ_o is mean of observations, and S_e is standard error of observed values. The 95 % confidence intervals (%) were estimated as mean $\pm RMSE_{95\%}$, with non-overlapping intervals indicating significant differences.

It is worth noting that this is not an evaluation of RothC, as the plant inputs were adjusted to fit the measured data, but it provides an estimate of the expected uncertainty in the simulations compared to measured values. This can then be used to estimate of model uncertainty in the long-term simulations.

2.5. Coupling HYDRUS with RothC model

To better account for future changes in soil hydrology, and so improve future C simulations, RothC was coupled with HYDRUS by replacing the model's default soil water accounting method with simulated VWC values from HYDRUS. Rather than relying on RothC's simplified monthly water balance method, daily soil VWC outputs from HYDRUS were cumulated to provide monthly values. These values were then used as direct inputs to drive the soil water modifier function in RothC, which controls the rate of organic matter decomposition. This approach allowed for a more realistic representation of soil water dynamics, especially under different climatic and cropping conditions. This coupling was applied across both cropping systems (barley monoculture and intercropping) under short-term and long-term future scenarios.

3. Results

3.1. Short-term water and carbon model performance

HYDRUS effectively captured both temporal and spatial soil water dynamics in the short-term. The optimised soil hydraulic parameter

values are given in Table 1. The values were similar across depths except K_s which reflect active root zone. The model's performance was tested against observed soil VWC. Soil water simulations generally agreed well with observation, showing optimal model performance. For calibration, the model achieved R^2, *RMSE* and *KGE* of 0.76, 3 %, 0.83 at 10 cm; 0.71, 3 %, 0.70 at 20 cm; and 0.82, 2 %, 0.71 at 30 cm depths, respectively (Fig. 2). Also, the model performed optimally during the evaluation period, as reflected by high R^2 (0.98), low *RMSE* (1 %), and high *KGE* (0.77) at 5 cm depth, though it is worth noting that this was calculated based on five values (Fig. 2). It was notable that the model tended to overestimate and underestimate soil water in 20 cm and 30 cm depths, respectively during the summer in 2023.

In addition to soil water dynamics, HYDRUS performance was tested against barley root water uptake patterns quantified as proportional soil water sources to water uptake. The model generally captured the water uptake patterns from both upper and lower topsoil layers in barley monoculture and intercropping systems, aligning with the mixing modelling results from isotope sampling observations (Fig. 3). However, the model tended to underestimate the proportions of water uptake from the upper topsoil compared to isotope observations, particularly during the dry period in June 2023. During the June 2023 sampling, the model indicated that barley in both monoculture and intercropping potentially showed greater reliance on lower topsoil water than was suggested by the isotope observations.

RothC effectively simulated the observed soil C stock dynamics in the upper topsoil in the short-term in both barley monoculture and intercropping. For monoculture, the model had R^2 of 0.95, *RMSE* of 0.05 kg m^{-2} (3.5 %) (which is less than $RMSE_{95\%}$ of 6.0 %) and *KGE* of 0.95. For intercropping, the model also had R^2 of 0.98, *RMSE* of 0.04 kg m^{-2} (2.6 %) (which is less than $RMSE_{95\%}$ of 6.4 %) and *KGE* 0.94. Values of *RMSE* (as a percentage of the average observed value) less than $RMSE_{95\%}$ indicate that predictions are within the 95 % confidence interval of the observations. This reflects the model's ability to fit measured data, but we could not complete an independent evaluation due to lack of independent data. It is worth reiterating that the intercropping was simulated based on only four values, and that the plant inputs were adjusted to ensure good model fit. Therefore, while these statistics provide an estimate of uncertainty, they do not represent an independent evaluation of model performance.

3.2. Water dynamics in intercropping compared to barley monoculture

Simulated soil VWC in the short term (2022−2023) was similar between barley monoculture and intercropping systems (Fig. S5), confirming similar patterns as reported in Durodola et al. (2025). Average daily root water uptake rate for barley in monoculture and intercropping was 1.4 mm day^{-1} and 1.1 mm day^{-1}, respectively, peaking during summer (Table S5).

During the short-term period with observations (2022 - 2023), seasonal E_a of barley monoculture ranged from 166 to 251 mm, T_a ranged from 168 to 192 mm while ET_a ranged from 333 to 443 mm. For intercropping, E_a ranged from 230 to 261 mm, T_a ranged from 211 to 215 mm, while ET_a ranged from 441 to 476 mm. Compared to barley monoculture, intercropping increased mean E_a by 18 % (208 vs 245 mm), increased mean T_a by 18 % (180 vs 213 mm), leading to 18 % increase in ET_a (388 vs 458 mm) (Fig. 4). It is worth noting that the increase in ET_a in intercropping is strongly influenced by 2022, a particularly dry year.

Table 1
Calibrated soil hydraulic parameters of different soil layers.

Soil layer (cm)	θ_r (%)	θ_s (%)	α (cm^{-1})	n (–)	K_s (cm day^{-1})	l (–)
0–10	8.86	39.88	0.0888	1.64	8.40	0.50
10–20	8.86	39.88	0.0545	1.84	28.45	0.50
20–30	8.86	39.88	0.0405	1.61	40.49	0.50

In the long-term (2024–2050), seasonal E_a of barley monoculture ranged from 167 to 257 mm, while T_a ranged from 152 to 236 mm and ET_a ranged from 322 to 487 mm. For intercropping, E_a ranged from 175 to 233 mm, while T_a ranged from 227 to 263 mm, and ET_a ranged from 410 to 494 mm. It is worth noting that intercropping has a narrower range of fluctuations in E_a, T_a and ET_a, indicating less vulnerability to climatic variability (Fig. 4). Compared to barley monoculture, intercropping decreased mean E_a by 10 % (218 vs 194 mm), but increased mean T_a by 18 % (205 vs 241 mm), overall leading to similar values in ET_a (423 vs 435 mm), although these were relatively higher for intercropping than barley monoculture during dry years (Fig. 4).

In summary, across all years (i.e. 2022 - 2050), compared to barley monoculture, intercropping decreased mean E_a by 9 % (217 vs 198 mm), but increased mean T_a by 18 % (203 vs 239 mm), leading to similar ET_a (420 vs 436 mm) (Fig. 4). Specifically, under dry conditions, ET_a of intercropping was considerably higher than barley monoculture, while similar under normal and wet hydro-climatological years (Fig. 5). This indicates that intercropping has higher evapotranspiration compared to barley monoculture during drought conditions, suggesting that intercropping adaptively uses available soil water and is less vulnerable to dry spells.

Specifically in intercropping, mean simulated barley and pea transpiration were 165 mm and 73 mm, respectively. Also, ΔS was very similar across all years in both systems, but intercropping generally showed lower storage losses in dry years, leading to less deep percolation (Table S6).

3.3. Soil carbon dynamics in intercropping compared to barley monoculture

Simulated soil C dynamics in the short term (2022 - 2023) showed close agreement between observed and simulated values across both cropping systems. For intercropping, observed soil C increased slightly from 1.61 ($\pm$ 0.10) kg m^{-2} in 2022 to 1.77 ($\pm$ 0.11) kg m^{-2} in 2023, while simulated values followed a similar trend, increasing from 1.62 ($\pm$ 0.10) to 1.73 ($\pm$ 0.11) kg m^{-2} (Fig. 6). In the barley monoculture, observed soil C was 1.53 ($\pm$ 0.09) kg m^{-2} in 2022 and increased to 1.67 ($\pm$ 0.10) kg m^{-2} in 2023, while simulated soil C showed a smaller increase from 1.59 ($\pm$ 0.09) to 1.63 ($\pm$ 0.10) kg m^{-2}, indicating that the model effectively captured short-term dynamics of soil C under both systems. The difference in simulated soil C between the two systems reached 0.10 ($\pm$ 0.006) kg m^{-2} in 2050, corresponding to a 6 % higher C observed under intercropping compared to barley monoculture. The observed increase in soil C under intercropping highlights its potential benefits for enhancing soil C relative to barley monoculture in the short-term.

In the long-term (2024–2050), simulated soil C revealed contrasting trends between intercropping and barley monoculture systems. By the end of the simulation period in 2050, intercropping had accumulated substantially more soil C than barley monoculture (Fig. 6). In the intercropping, soil C increased steadily over the simulation period, rising from an initial value of 1.77 ($\pm$ 0.11) kg m^{-2} in 2023 to 1.91 ($\pm$ 0.12) kg m^{-2} by 2050, with overlapping 95 % confidence intervals (1.66 - 1.88 kg m^{-2} and 1.79 - 2.03 kg m^{-2}). The absolute difference represents a net gain of 0.14 ($\pm$ 0.009) kg m^{-2}. In contrast, the barley monoculture system exhibited a relatively stable trend, with soil C slightly declining from 1.67 ($\pm$ 0.10) to 1.63 ($\pm$ 0.10) kg m^{-2}, with overlapping 95 % confidence intervals (1.57 - 1.77 kg m^{-2} and 1.53 - 1.73 kg m^{-2}) during the same period (Fig. 6). The difference in soil C between the two systems reached 0.28 ($\pm$ 0.017) kg m^{-2} in 2050 (without overlapping 95 % confidence intervals from 2040), corresponding to a 16 % higher C under intercropping compared to barley monoculture (Fig. 6). This difference emerged gradually over the simulation period, with the gap widening as the benefits of intercropping accumulated over successive years. These results clearly show that the intercropping system was more helpful at enhancing soil C sequestration relative to barley monoculture under future climate. This suggests that cropping system had a strong
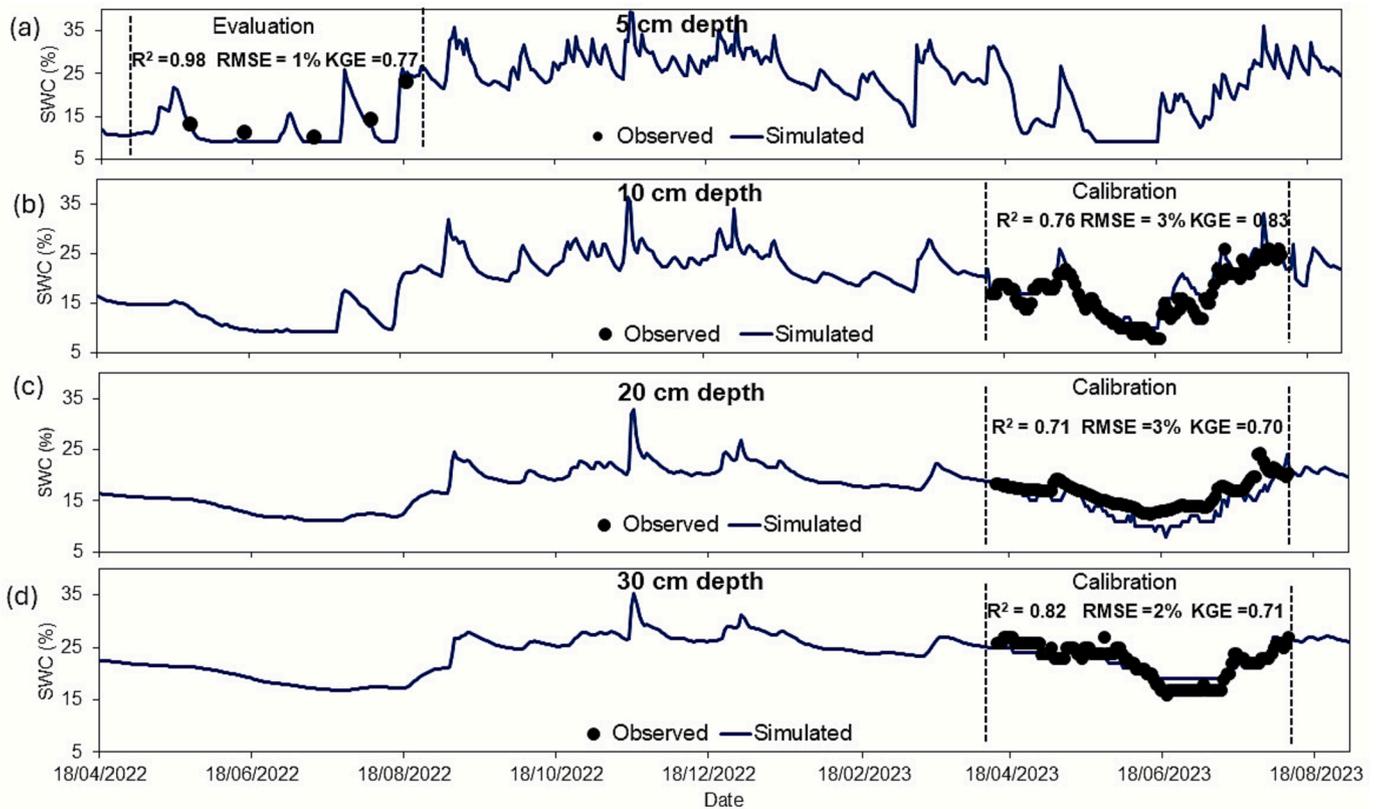
Fig. 2. a–d: Simulated and observed soil volumetric water content (VWC, %) for the barley monoculture in HYDRUS at 5, 10, 20, and 30 cm soil depths during the 2022 and 2023 growing seasons, with calibration and evaluation periods. Coefficient of determination (R^2) root mean square error (*RMSE*), and the Kling–Gupta Efficiency (*KGE*) performance criteria are shown.
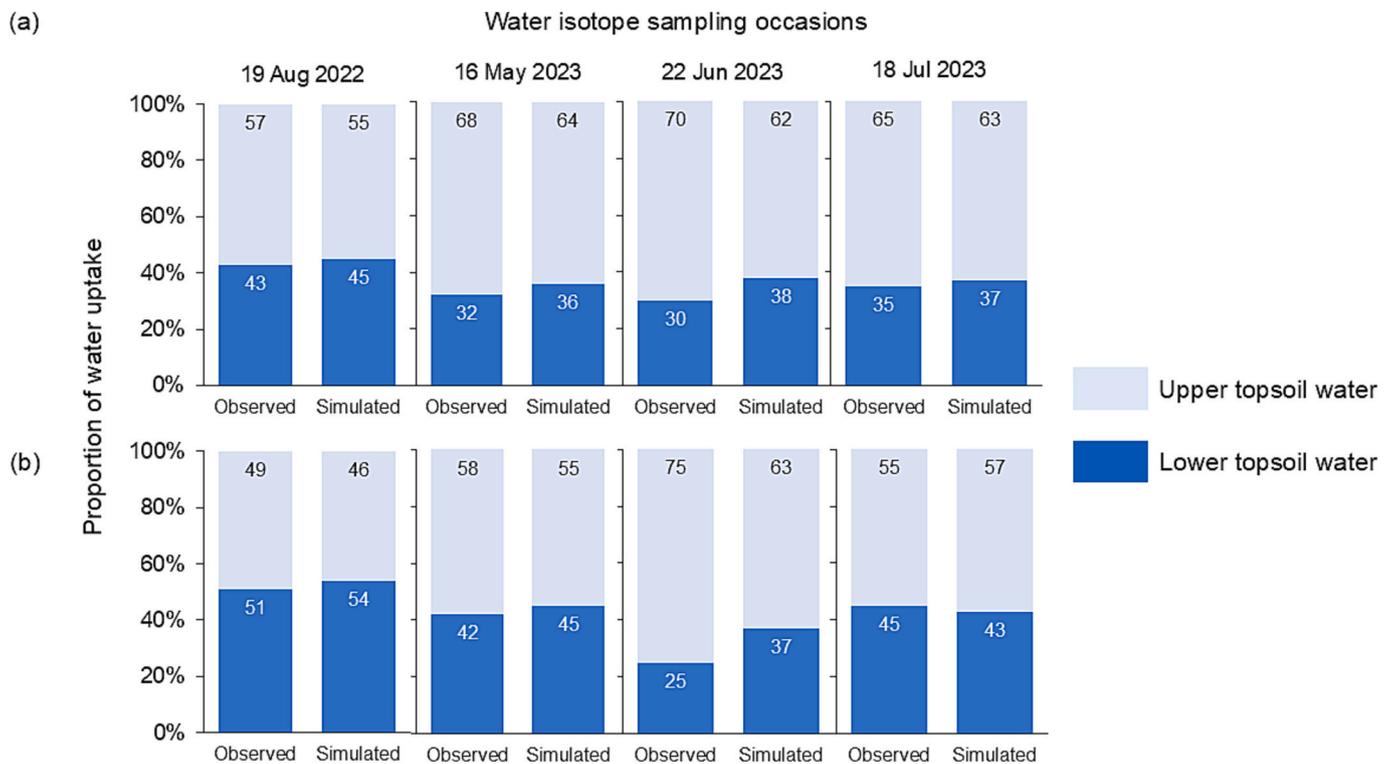

Fig. 3. Observed (Durodola et al., 2025) and simulated proportional contributions of soil water sources (upper topsoil, 0–5 cm; and lower topsoil, 5–30 cm) to barley water uptake in barley monoculture (a) and intercropping (b) during water isotope sampling occasions.
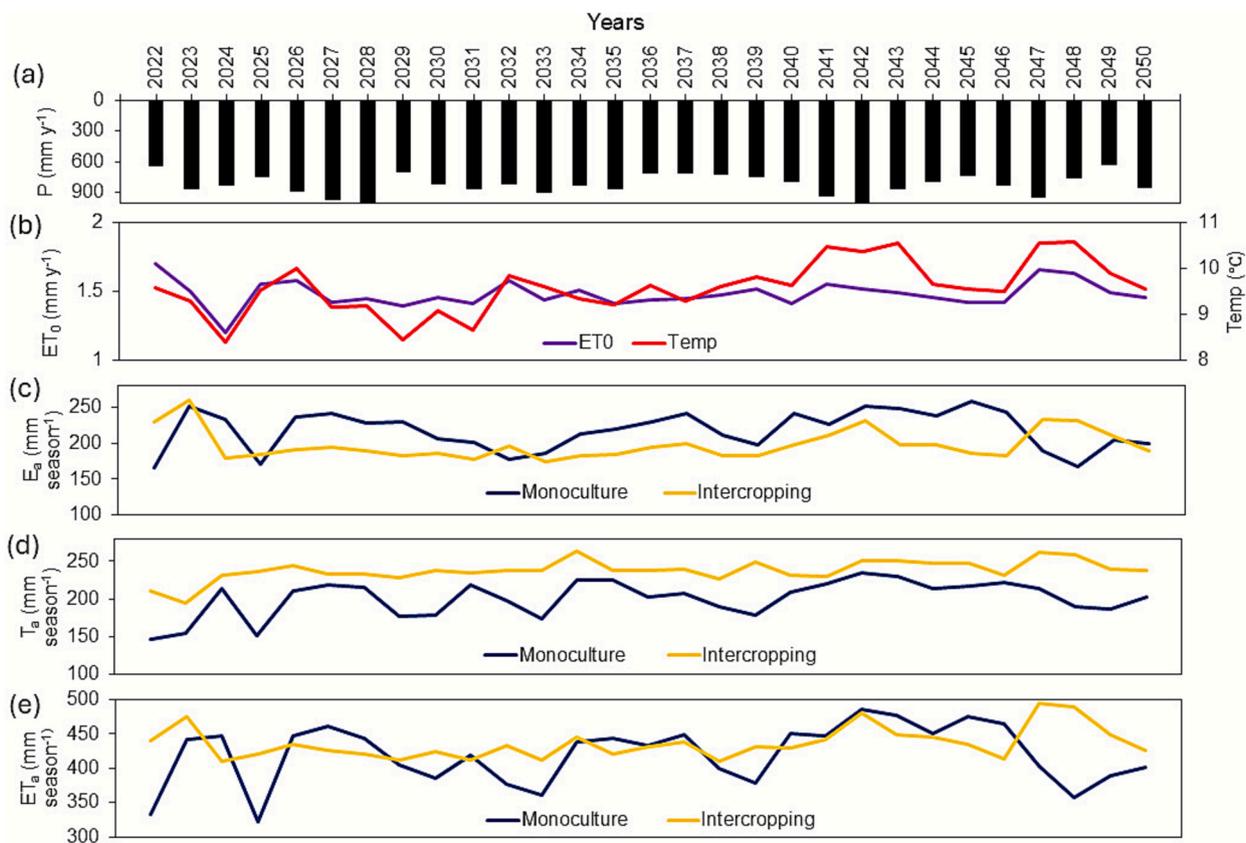
Fig. 4. Climatic and simulated water dynamics conditions for barley monoculture and intercropping. (a) Sum of annual (October–September) precipitation (P, mm yr^{-1}); (b) average annual (October–September) potential evapotranspiration (ET_0, mm y^{-1}) and average annual (October–September) air temperature (°C); (c) simulated seasonal (April–August) actual soil evaporation (E_a, mm season^{-1}); (d) simulated seasonal (April–August) actual transpiration (barley + pea) (T_a, mm season^{-1}); and (e) simulated seasonal (April–August) actual evapotranspiration (ET_a, mm season^{-1}).
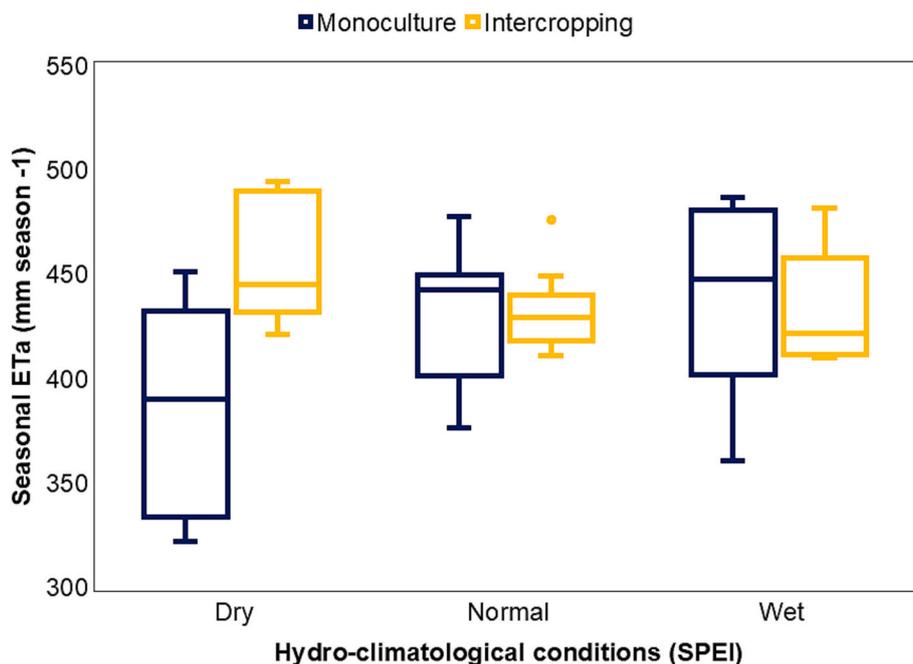

Fig. 5. Seasonal actual evapotranspiration (ET_a) of intercropping and barley monoculture across different hydro-climatological conditions (based on Standardised Precipitation and Evapotranspiration Index, SPEI). Each boxplot displays the median (line within the box), the interquartile range from the 25th to 75th percentiles, and outlier values.
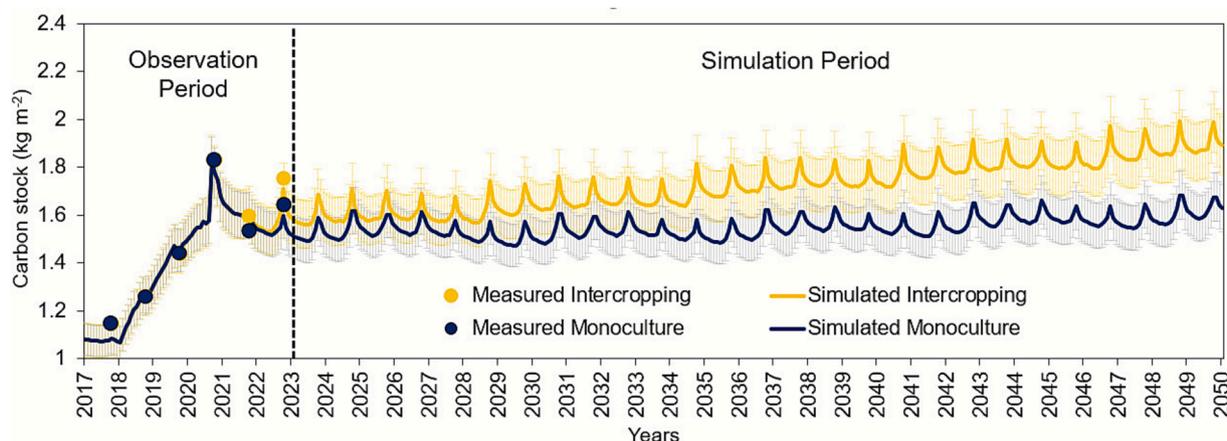
Fig. 6. Simulated and observed soil carbon stock (kg m^{-2}) in barley monoculture and intercropping in coupled HYDRUS-RothC using future climate projections. Note: error bars represent the average 95 % confidence interval observed in the trial reported in Durodola et al. (2026).

influence on soil C dynamics over time, with intercropping exhibiting consistent upward trend while barley monoculture remained similar.

4. Discussion

This research provides novel insights into long-term water and C dynamics in temperate barley-pea intercropping and barley monoculture systems under a worst-case (RCP 8.5) projected climate change scenario by coupling water (HYDRUS) and C (RothC) models. Overall, intercropping is projected to increase transpiration, but reduce evaporation, leading to similar evapotranspiration with barley monoculture during wet years, although with higher evapotranspiration during dry years. Also, intercropping is projected to increase soil C storage in the upper topsoil compared to barley monoculture by 2050.

4.1. Coupled water-carbon modelling performance

Overall, the coupled water and C modelling in HYDRUS-RothC demonstrated a good performance in simulating short-term soil water and C dynamics, effectively capturing observed changes in both intercropping and barley monoculture systems. Over the short-term, the modelling closely agreed with observed measurements, reflecting spatial and temporal patterns in water and C dynamics across both systems. These findings suggest that a coupled approach of HYDRUS and RothC is capable of accurately representing soil water and C dynamics, respectively, providing valuable insights into water movement and C accumulation in agroecosystems (Chen et al., 2022b). It is worth noting that future observations of actual transpiration and evaporation would also help to further evaluate the modelling. HYDRUS's over- and under-estimation at certain depths likely reflects uncertainties in root density parameterisation (Šimůnek et al., 2024), suggesting that refining root profiles in future studies could improve depth-specific model performance. In addition, an independent evaluation of the simulations of C accumulation is needed to demonstrate efficacy of the model at different sites.

For long-term simulations, the coupling of HYDRUS-simulated soil moisture into RothC also proved critical in capturing the dynamic interactions between water availability and soil C cycling. Soil VWC is a key driver of microbial activity, decomposition rates, and organic matter stabilisation (Wang et al., 2024b); thus, simulating its spatiotemporal variability allowed RothC to capture the effects of water stress or excess water on soil C sequestration under different cropping systems. This coupled approach offered a more process-based representation and understanding of how soil water interacts with C sequestration under monoculture versus intercropping and different climate conditions (Chen et al., 2022b; Wang et al., 2024b). Notably, this coupling allowed

for better sensitivity to climatic variability and provided enhanced insight into system-specific soil water and C dynamics over the long-term.

However, soil C in this study was assessed only in the upper 5 cm of the soil profile, which, while appropriate for capturing upper topsoil dynamics, may not fully represent the vertical distribution and stabilisation potential of C at lower topsoil. Future studies could consider exploring the effects of intercropping on C in deeper soil depths, particularly given the importance of deeper C pools in long-term sequestration processes and ecosystem services (Yu et al., 2022). It is acknowledged that not including pea monoculture in this study prevented a balanced comparison of monocultures with the intercropping system, though barley monoculture is the dominant baseline to compare against in this environment. Future studies should aim to incorporate both cereal and legume monocultures to enable a more comprehensive assessment of intercropping performance. Furthermore, the interpolation of RothC relied on a relatively short duration (two years) of observed intercropping results which may limit the robustness of model parameterisation for this cropping system. Additional long-term field data from diverse intercropping systems would strengthen model performance, provide more insights into C sequestration in deeper soil layers and enhance reliability on future long-term projections.

4.2. Role of intercropping in water cycling under climate change

In this study, the simulated water use under intercropping revealed key hydrological differences when compared to barley monoculture. Across all years, intercropping showed increased plant transpiration, decreased soil evaporation, and similar evapotranspiration, although the latter was higher during drier years. Overall, soil water storage under the intercropping system was also similar to that under barley monoculture, as observed in several other intercropping studies (Fan et al., 2016; Liu et al., 2025; Yin et al., 2020). The observed shift from non-productive water loss (evaporation) to productive water use (transpiration) under intercropping can be attributable to better vegetative cover of the ground surface in intercropping due to the complementarity in plant architectures between the cereal and legume (Fan et al., 2016). This shift to productive water use in intercropping underscores its potential to improve water use patterns without depleting total soil water storage. Importantly, such partitioning of water fluxes enhances productive water use by channelling water toward physiological functions that support improved biomass production and higher yield in intercropping (Rahman et al., 2017; Stomph et al., 2020). This partitioning was particularly observed under drought conditions, where more adaptive use of water could help sustain yield stability (Yin et al., 2020).

The simulated increase in evapotranspiration for intercropping

under drought conditions is largely driven by higher plant transpiration and may be attributed to root water uptake plasticity. Root water uptake plasticity refers to the ability of plant roots to adjust the water acquisition patterns in response to variability in soil water availability and environmental conditions (Fromm, 2019). Intercropped plants could facilitate deeper water uptake through root water uptake plasticity, allowing water acquisition from deeper sources where water is available during drought (Durodola et al., 2025). Moreover, intercropping influences soil water dynamics through complementary belowground water uptake by root systems, thereby exploiting soil water layers differently (Yin et al., 2020). This strategy implies less vulnerability of intercropping to drought and could reduce the reliance on irrigation under projected future climate, while offering economic and environmental benefits.

Intercropping was observed to reduce soil evaporation compared to barley monoculture which could be attributed to less gappy soil cover in intercropping (Rahman et al., 2017). This denser canopy cover was quantitatively captured in HYDRUS through the combination of the *LAI* of barley and pea in intercropping. Although intercropping may have exhibited a slightly higher (~4 %) total evapotranspiration than barley monoculture, it did not lead to over-exploitation of water; this is due to a more balanced seasonal soil water storage. Moreover, it should be noted that these simulated increases are small and likely to be within the expected range of uncertainty associated with limitations in data and model structure, parameterisation and calibration. Overall, the seasonal distribution of soil water remained less variable under intercropping, with adaptive capture and use of available water throughout the growing period. This highlights the system's ability to sustain soil water availability while maintaining productivity, contributing to long-term water sustainability (Liu et al., 2025).

It is acknowledged that this study is limited to a single climate emissions pathway. It is notable that the impacts of climate change tend to remain relatively consistent across low and high scenarios until mid-century (2040 - 2050), after which substantial divergence emerges (IPCC, 2023). Future research should therefore explore the impact of intercropping on water dynamics under a wider range of projected future climate scenarios (e.g., RCP 4.5 and RCP 6.0) and up to the late century. Integrating these long-term projections with system-specific intercropping designs could help further refine adaptation strategies for sustainable water management.

4.3. Role of intercropping in long-term soil C sequestration

Relatively steady soil C was simulated under barley monoculture over the study period (~25 years). Declines in soil C in monocultures may occur over longer timescales as suggested by Prudil et al. (2023), who projected C loss in continuous barley monoculture systems over the long-term (~80 years) under climate change in temperate environments, attributable to the decline in organic matter inputs and reduced belowground biomass returns. These findings emphasise the concern that continuous monocropping, especially of non-leguminous species, could lead to a gradual depletion of soil C stocks over time, with implications for both soil fertility and long-term sustainability of cereal monoculture systems (Smith et al., 2007). On the other hand, the increase in soil C under intercropping observed in this study is similar to the findings of Li et al. (2024) and Wang et al. (2025a), who found improved soil C accumulation under intercropping in a global synthesis and a 7-year field experiment in China, respectively. While direct comparisons with intercropping studies in temperate environments are limited, similar increased C effects have been found in diversified farming systems such as cover cropping and agroforestry. For instance, Begum et al. (2022) and Smith et al. (2007) projected enhanced soil C in diversified systems relative to monocultures, highlighting the broader potential of biodiversity driven approaches to improve soil C.

The increased soil C under intercropping in the short-and long-term could be attributable to enhanced aboveground biomass production. Higher aboveground biomass is likely to have resulted in greater plant residue inputs to the soil, particularly from pea in the intercrop, a nitrogen fixing legume, which could subsequently contribute to the increase in soil C levels (Li et al., 2024; Wang et al., 2025a). Plant residues enhance soil organic matter through plant material decomposition, thus increasing soil C stocks (Yu et al., 2022). In addition, intercropping promotes enhanced root biomass and deeper root systems, which increase root-derived C inputs and belowground biomass (Li et al., 2024; Stomph et al., 2020). Root exudation in intercrops has also been shown to stimulate microbial activity and contribute to the transformation and stabilisation of rhizosphere C while contributing to increased C inputs, nutrient cycling and plant growth (Wang et al., 2025b; Yu et al., 2022). Intercropping promotes diverse microbial communities that enhance nutrient availability and cycling (Wang et al., 2025b), contributing to better soil fertility which could reduce the need for agrochemical inputs.

While the current results underscore the potential of intercropping to enhance soil C in temperate environments, further research is necessary to evaluate its long-term crop productivity and overall viability. Specifically, assessing yield (stability), resource use efficiency, economic productivity and suitability of seed for end uses (e.g. distilling), overall nutrient (e.g. nitrogen, phosphorus) cycling, and socio-economic benefits of different crop combinations will be essential to identify viable and sustainable intercropping designs for temperate environments.

4.4. Broader implications

This study revealed that over the long-term under a projected worst-case climate scenario, intercropping would likely have similar evapotranspiration rates during wet years compared to barley monoculture, but higher evapotranspiration during drought years. However, during these drier years, a shift from unproductive water loss through evaporation toward beneficial transpiration was observed, directly contributing to crop growth. Moreover, the intercropping system showed less interannual variability to climate change and higher adaptive water use during dry years (Fig. 5), indicating its potential as a climate-resilient strategy under projected climate change. Intercropping might be beneficial for the food and drink industries which require stable and predictable yields, while also reducing the need for irrigation under extremely dry summers (Glendell et al., 2024).

Although this study focused on a worst-case climate scenario, it is expected that intercropping would still provide hydrological resilience and not cause overexploitation of water as shown during normal years. This is consistent with the underlying mechanisms driving these benefits in intercropping systems. Thus, the findings of this study support the potential of intercropping as a climate-resilient strategy across a range of future climate trajectories.

Intercropping is also projected to enhance long-term soil C. These gains could improve soil structure, water holding capacity, nutrient cycling, and microbial activity, supporting wider ecosystem functions (Wang et al., 2025b; Yu et al., 2022). Enhanced soil C sequestration also suggest the potential of intercropping for integration into C credit schemes and agri-environmental schemes, offering farmers financial incentives while contributing to net-zero targets (Raina et al., 2024). The projected C benefits also strengthen the case for policy support as part of national climate and soil health strategies.

Intercropping could be combined with other nature-based solutions such as minimum tillage, cover cropping, and crop diversification, to reduce reliance on chemical input, promote soil health and biodiversity while adapting to climate change (Hawes et al., 2018). Policy frameworks that promote intercropping through agri-environmental payments, extension services, or C markets can, therefore, help to drive the transition toward more sustainable land management in temperate environments.

5. Conclusions

This research provides insights into long-term water and C dynamics in temperate barley-pea intercropping and barley monoculture systems under a worst-case (RCP 8.5) projected climate change scenario. Water and C dynamics were projected for the short-term (2022 - 2023) and long-term (2024 - 2050) by coupling well known HYDRUS and RothC water and C models, respectively. Across all years, compared to barley monoculture, intercropping reduced soil evaporation, but increased plant transpiration. Evapotranspiration in intercropping was similar to barley monoculture, but increased because of relatively higher transpiration during dry years, indicating potential hydrological resilience and adaptive water use. Intercropping also showed lower inter-annual fluctuations in water use, indicating less vulnerability to climatic variability. Intercropping is also projected to increase soil C in the upper topsoil (0 - 5 cm) by 16 % compared to barley monoculture (1.91 ± 0.12 vs 1.63 ± 0.10 kg m^{-2}) by 2050. These novel findings reveal the potential of intercropping for long-term environmental sustainability and C sequestration in temperate environments and suggest that intercropping could potentially contribute to sustainable environmental management, climate change adaptation and mitigation policies.

CRediT authorship contribution statement

Oludare S. Durodola: Writing – review & editing, Writing – original draft, Visualization, Validation, Software, Project administration, Methodology, Investigation, Funding acquisition, Formal analysis, Data curation, Conceptualization. **Cathy Hawes:** Writing – review & editing, Supervision, Resources, Methodology, Investigation, Funding acquisition, Conceptualization. **Jo Smith:** Writing – review & editing, Validation, Supervision, Resources, Methodology, Investigation, Funding acquisition, Conceptualization. **Tracy A. Valentine:** Writing – review & editing, Supervision, Resources, Methodology, Investigation, Funding acquisition, Conceptualization. **Josie Geris:** Writing – review & editing, Validation, Supervision, Resources, Project administration, Methodology, Investigation, Funding acquisition, Conceptualization.

Funding

Declaration of competing interest

The authors declare that they have no known competing financial interests or personal relationships that could have appeared to influence the work reported in this paper.

Acknowledgements

Appendix A. Supplementary data

Supplementary data to this article can be found online at https://doi.org/10.1016/j.scitotenv.2025.181060.

Data availability

No data was used for the research described in the article.

References

Allen, R.G., Pereira, L.S., Raes, D., Smith, M., 1998. Crop Evapotranspiration: Guidelines for Computing Crop Water Requirements.

Baruth, B., Bettio, M., Chukaliev, O., Bojanowski, J., Bussay, A., Duveiller, G., Fontana, G., Kasperska-Wolowicz, W., Lopez, R., Maiorano, A., Seguini, L., Srivastava, A., 2012. Crop monitoring in Europe. In: MARS Bulletin, Vol. 20 (No. 7. https://publications.jrc.ec.europa.eu/repository/bitstream/JRC68570/lb-am-12-007-en-n.pdf).

Begum, K., Zornoza, R., Farina, R., Lemola, R., Álvaro-Fuentes, J., Cerasuolo, M., 2022. Modeling soil carbon under diverse cropping systems and farming management in contrasting climatic regions in Europe. Front. Environ. Sci. 10, 819162. https://doi.org/10.3389/FENVS.2022.819162.

Belmans, C., Wesseling, J.G., Feddes, R.A., 1983. Simulation model of the water balance of a cropped soil: SWATRE. J. Hydrol. 63 (3–4), 271–286. https://doi.org/10.1016/0022-1694(83)90045-8.

Brooker, R.W., Pakeman, R.J., Adam, E., Banfield-Zanin, J.A., Bertelsen, I., Bickler, C., Fog-Petersen, J., George, D., Newton, A.C., Rubiales, D., Tavoletti, S., Villegas-Fernández, Á.M., Karley, A.J., 2024. Positive effects of intercrop yields in farms from across Europe depend on rainfall, crop composition, and management. Agron. Sustain. Dev. 44 (4), 1–12. https://doi.org/10.1007/S13593-024-00968-2.

Chen, N., Li, X., Šimůnek, J., Shi, H., Hu, Q., Zhang, Y., 2020. Evaluating soil nitrate dynamics in an intercropping dripped ecosystem using HYDRUS-2D. Sci. Total Environ. 718, 137314. https://doi.org/10.1016/J.SCITOTENV.2020.137314.

Chen, N., Li, X., Šimůnek, J., Shi, H., Zhang, Y., Hu, Q., 2022a. Quantifying inter-species nitrogen competition in the tomato-corn intercropping system with different spatial arrangements. Agr. Syst. 201, 103461. https://doi.org/10.1016/J.AGSY.2022.103461.

Chen, Y., Wei, T., Ren, K., Sha, G., Guo, X., Fu, Y., Yu, H., 2022b. The coupling interaction of soil organic carbon stock and water storage after vegetation restoration on the Loess Plateau, China. J. Environ. Manag. 306, 114481. https://doi.org/10.1016/J.JENVMAN.2022.114481.

Coleman, K., Jenkinson, D., 2024. RothC - a model for the turnover of carbon in soil – model description. https://www.rothamsted.ac.uk/sites/default/files/Documents/RothC_description.pdf.

Coleman, K., Jenkinson, D.S., 1996. RothC-26.3 - a model for the turnover of carbon in soil. In: Evaluation of Soil Organic Matter Models, pp. 237–246. https://doi.org/10.1007/978-3-642-61094-3_17.

Cong, W.F., Hoffland, E., Li, L., Six, J., Sun, J.H., Bao, X.G., Zhang, F.S., Van Der Werf, W., 2015. Intercropping enhances soil carbon and nitrogen. Glob. Chang. Biol. 21 (4), 1715–1726. https://doi.org/10.1111/GCB.12738.

Durodola, O.S., Binnie, K., Hawes, C., Smith, J., Valentine, T.A., Geris, J., 2026. Effects of barley-pea intercropping on soil carbon, crop productivity and grain quality in a low-input temperate agroecosystem. Agron. J. (in press).

Durodola, O.S., Rothfuss, Y., Hawes, C., Smith, J., Valentine, T.A., Geris, J., 2025. Stable water isotopes reveal modification of cereal water uptake strategies in agricultural co-cropping systems. Agr Ecosyst Environ 381, 109439. https://doi.org/10.1016/J.AGEE.2024.109439.

Ehret, U., Zehe, E., Wulfmeyer, V., Warrach-Sagi, K., Liebert, J., 2012. HESS opinions "should we apply bias correction to global and regional climate model data?". Hydrol. Earth Syst. Sci. 16 (9), 3391–3404. https://doi.org/10.5194/HESS-16-3391-2012.

Falloon, P., Smith, P., Coleman, K., Marshall, S., 1998. Estimating the size of the inert organic matter pool from total soil organic carbon content for use in the Rothamsted carbon model. Soil Biol. Biochem. 30 (8–9), 1207–1211. https://doi.org/10.1016/S0038-0717(97)00256-3.

Fan, Z., An, T., Wu, K., Zhou, F., Zi, S., Yang, Y., Xue, G., Wu, B., 2016. Effects of intercropping of maize and potato on sloping land on the water balance and surface runoff. Agric Water Manag 166, 9–16. https://doi.org/10.1016/J.AGWAT.2015.12.006.

Feddes, R., Kowalik, P., Zaradny, H., 1978. Simulation of Field Water Use and Crop Yield. John Wiley & Sons.

Fromm, H., 2019. Root plasticity in the pursuit of water. Plants 8 (7), 236. https://doi.org/10.3390/PLANTS8070236.

Geris, J., Verrot, L., Gao, L., Peng, X., Oyesiku-Blakemore, J., Smith, J.U., Hodson, M.E., McKenzie, B.M., Zhang, G., Hallett, P.D., 2021. Importance of short-term temporal variability in soil physical properties for soil water modelling under different tillage practices. Soil Tillage Res. 213, 105132. https://doi.org/10.1016/J.STILL.2021.105132.

Glendell, M., Blackstock, K., Adams, K., Brickell, J., Comte, J.-C., Gagkas, Z., Geris, J., Haro, D., Jabloun, M., Karley, A., Kuhfuss, L., Macleod, K., Naha, S., Paterson, E., Rivington, M., Thompson, C., Upton, K., Wilkinson, M., Williams, K., 2024. Future predictions of water scarcity in Scotland: impact on distilleries and agricultural abstractors. https://www.crew.ac.uk/sites/www.crew.ac.uk/files/publication/CRW2023_05_Main_report_and_appendices_FINAL_V2.pdf.

Gupta, H.V., Kling, H., Yilmaz, K.K., Martinez, G.F., 2009. Decomposition of the mean squared error and NSE performance criteria: implications for improving hydrological modelling. J. Hydrol. 377 (1–2). https://doi.org/10.1016/j.jhydrol.2009.08.003.

Hawes, C., Alexander, C.J., Begg, G.S., Iannetta, P.P.M., Karley, A.J., Squire, G.R., Young, M., 2018. Plant responses to an integrated cropping system designed to

maintain yield whilst enhancing soil properties and biodiversity. Agronomy 8 (10), 229. https://doi.org/10.3390/AGRONOMY8100229.

IPCC, 2023. Summary for policymakers. In: Core Writing Team, Lee, H., Romero, J. (Eds.), Climate Change 2023: Synthesis Report. Contribution of Working Groups I, II and III to the Sixth Assessment Report of the Intergovernmental Panel on Climate Change. IPCC. https://doi.org/10.59327/IPCC/AR6-9789291691647.001.

Lazarovitch, N., Poulton, M., Furman, A., Warrick, A.W., 2009. Water distribution under trickle irrigation predicted using artificial neural networks. J. Eng. Math. 64 (2), 207–218. https://doi.org/10.1007/S10665-009-9282-2.

Li, S., Ye, S., Liu, Z., Hassan, M.U., Huang, G., Zhou, Q., 2024. How does intercropping contribute to soil organic carbon accumulation? A global synthesis. Agr Ecosyst Environ 374, 109173. https://doi.org/10.1016/J.AGEE.2024.109173.

Liu, H., Gao, X., Li, C., Cai, Y., Song, X., Zhao, X., 2025. Intercropping increases plant water availability and water use efficiency: a synthesis. Agr Ecosyst Environ 379, 109360. https://doi.org/10.1016/J.AGEE.2024.109360.

Prudil, J., Pospíšilová, L., Dryšlová, T., Barančíková, G., Smutný, V., Sedlák, L., Ryant, P., Hlavinka, P., Trnka, M., Halas, J., Koco, Š., Takáč, J., Boturová, K., Dušková, S., Neudert, L., Rábek, M., 2023. Assessment of carbon sequestration as affected by different management practices using the RothC model. Plant Soil Environ. 69 (11), 532–544. https://doi.org/10.17221/291/2023-PSE.

Rahman, T., Liu, X., Hussain, S., Ahmed, S., Chen, G., Yang, F., Chen, L., Du, J., Liu, W., Yang, W., 2017. Water use efficiency and evapotranspiration in maize-soybean relay strip intercrop systems as affected by planting geometries. PloS One 12 (6), e0178332. https://doi.org/10.1371/JOURNAL.PONE.0178332.

Raina, N., Zavalloni, M., Viaggi, D., 2024. Incentive mechanisms of carbon farming contracts: a systematic mapping study. J. Environ. Manage. 352, 120126. https://doi.org/10.1016/J.JENVMAN.2024.120126.

Reyniers, N., Addor, N., Zha, Q., Osborn, T., Forstenhäusler, N., He, Y., 2022a. UKCP18 RCM Precipitation and Temperature Bias Corrected Using ISIMIP3BA Change-preserving Quantile Mapping. https://doi.org/10.5281/ZENODO.6337381.

Reyniers, N., Osborn, T., Addor, N., Darch, G., 2022b. Projected Changes in Droughts and Extreme Droughts in Great Britain Are Strongly Influenced by the Choice of Drought Index: UKCP18-based Bias Adjusted Potential Evapotranspiration. https://doi.org/10.5281/ZENODO.6320707.

Reyniers, N., Zha, Q., Addor, N., Osborn, T.J., Forstenhäusler, N., He, Y., 2025. Two sets of bias-corrected regional UK Climate Projections 2018 (UKCP18) of temperature, precipitation and potential evapotranspiration for Great Britain. Earth Syst. Sci. Data 17 (5), 2113–2133. https://doi.org/10.5194/ESSD-17-2113-2025.

Robertson, M.J., Silim, S., Chauhan, Y.S., Ranganathan, R., 2001. Predicting growth and development of pigeonpea: biomass accumulation and partitioning. Field Crop Res 70 (2), 89–100. https://doi.org/10.1016/S0378-4290(01)00125-3.

Rodriguez, C., Carlsson, G., Englund, J.E., Flöhr, A., Pelzer, E., Jeuffroy, M.H., Makowski, D., Jensen, E.S., 2020. Grain legume-cereal intercropping enhances the use of soil-derived and biologically fixed nitrogen in temperate agroecosystems. A meta-analysis. Eur. J. Agron. 118, 126077. https://doi.org/10.1016/J.EJA.2020.126077.

Schaap, M.G., Leij, F.J., Van Genuchten, M.T., 2001. rosetta: a computer program for estimating soil hydraulic parameters with hierarchical pedotransfer functions. J. Hydrol. 251 (3–4), 163–176. https://doi.org/10.1016/S0022-1694(01)00466-8.

Šimůnek, J., van Genuchten, M.T., 1999. Using the hydrus-1D and hydrus-2D codes for estimating unsaturated soil hydraulic and solute transport parameters. In: van Genuchten, M.Th., Leij, F.J., Wu, L. (Eds.), Characterization and Measurement of the Hydraulic Properties of Unsaturated Porous Media. University of California, pp. 1523–1536.

Šimůnek, J., Brunetti, G., Jacques, D., van Genuchten, M.T., Šejna, M., 2024. Developments and applications of the HYDRUS computer software packages since 2016. Vadose Zone J. 23 (4), e20310. https://doi.org/10.1002/VZJ2.20310.

Smith, P., Smith, J.U., Powlson, D.S., McGill, W.B., Arah, J.R.M., Chertov, O.G., Coleman, K., Franko, U., Frolking, S., Jenkinson, D.S., Jensen, L.S., Kelly, R.H., Klein-Gunnewiek, H., Komarov, A.S., Li, C., Molina, J.A.E., Mueller, T., Parton, W.J., Thornley, J.H.M., Whitmore, A.P., 1997. A comparison of the performance of nine soil organic matter models using datasets from seven long-term experiments. Geoderma 81 (1–2), 153–225. https://doi.org/10.1016/S0016-7061(97)00087-6.

Smith, P., Smith, J.U., Franko, U., Kuka, K., Romanenkov, V.A., Shevtsova, L.K., Wattenbach, M., Gottschalk, P., Sirotenko, O.D., Rukhovich, D.I., Koroleva, P.V., Romanenko, I.A., Lisovoi, N.V., 2007. Changes in mineral soil organic carbon stocks in the croplands of European Russia and the Ukraine, 1990-2070; comparison of three models and implications for climate mitigation. Reg. Environ. Chang. 7 (2), 105–119. https://doi.org/10.1007/S10113-007-0028-2.

Šimůnek, J., Van Genuchten, Šejna, M., Šimůnek, J., Zone, V., 2016. Recent developments and applications of the HYDRUS computer software packages. Vadose Zone J. 15 (7), 1–25. https://doi.org/10.2136/VZJ2016.04.0033.

Smith, R., Antoniou, V., Askquith-Ellis, A., Ball, L.A., Bennett, E.S., Blake, J.R., Boorman, D.B., Brooks, M., Clarke, M., Cooper, H.M., Cowan, N., Cumming, A., Evans, J.G., Farrand, P., Fry, M., Harvey, D., Houghton-Carr, H., Howson, T., Jiménez-Arranz, G., Keen, Y., Khamis, D., Leeson, S., Lord, W.D., Morrison, R., Nash, G.V. (Eds.), 2024. Daily and Sub-Daily Hydrometeorological and Soil Data (2013–2023) [COSMOS-UK]. NERC EDS Environmental Information Data Centre. https://doi.org/10.5285/399ed9b1-bf59-4d85-9832-ee4d29f49bfb.

Stomph, T.J., Dordas, C., Baranger, A., de Rijk, J., Dong, B., Evers, J., Gu, C., Li, L., Simon, J., Jensen, E.S., Wang, Q., Wang, Y., Wang, Z., Xu, H., Zhang, C., Zhang, L., Zhang, W.P., Bedoussac, L., van der Werf, W., 2020. Designing intercrops for high yield, yield stability and efficient use of resources: are there principles? Adv. Agron. 160 (1), 1–50. https://doi.org/10.1016/BS.AGRON.2019.10.002.

van Genuchten, M.Th., 1980. A closed-form equation for predicting the hydraulic conductivity of unsaturated soils. Soil Sci. Soc. Am. J. 44 (5), 892–898. https://doi.org/10.2136/SSSAJ1980.03615995004400050002X.

Vicente-Serrano, S.M., Beguería, S., López-Moreno, J.I., 2010. A multiscalar drought index sensitive to global warming: the standardized precipitation evapotranspiration index. J. Climate 23 (7), 1696–1718. https://doi.org/10.1175/2009JCLI2909.1.

Visser-Quinn, A., Beevers, L., Lau, T., Gosling, R., 2021. Mapping future water scarcity in a water abundant nation: near-term projections for Scotland. Clim. Risk Manag. 32, 100302. https://doi.org/10.1016/J.CRM.2021.100302.

Wang, W., Li, M.Y., Wang, Y., Li, J.M., Zhang, W., Wen, Q.H., Huang, S.J., Chen, G.R., Zhu, S.G., Wang, J., Ullah, F., Xiong, Y.C., 2025a. Legume intercropping improves soil organic carbon stability in drylands: a 7-year experimental validation. Agr Ecosyst Environ 381, 109456. https://doi.org/10.1016/J.AGEE.2024.109456.

Wang, W., Li, M.Y., Wen, Q.H., Mo, F., Ren, A.T., Duan, H.X., Tao, H.Y., Li, J.M., Cao, J., Sheteiwy, M.S., Xiong, Y.C., 2025b. Plant-plant interactions drive the decomposition of soil organic carbon via nutrition competition in dryland. Plant Cell Environ. 48 (7), 4756–4769. https://doi.org/10.1111/PCE.15472.

Wang, X., Li, Y., Biswas, A., Sang, H., He, J., Liu, D.L., Yu, Q., Feng, H., Siddique, K.H.M., 2024a. Modeling soil water and salt dynamics in cotton-sugarbeet intercropping and their monocultures with biochar application. Soil Tillage Res. 240, 106070. https://doi.org/10.1016/J.STILL.2024.106070.

Wang, Y.P., Zhang, L., Liang, X., Yuan, W., 2024b. Coupled models of water and carbon cycles from leaf to global: a retrospective and a prospective. Agric. For. Meteorol. 358, 110229. https://doi.org/10.1016/J.AGRFORMET.2024.110229.

Yin, W., Chai, Q., Zhao, C., Yu, A., Fan, Z., Hu, F., Fan, H., Guo, Y., Coulter, J.A., 2020. Water utilization in intercropping: a review. Agric Water Manag 241, 106335. https://doi.org/10.1016/J.AGWAT.2020.106335.

Yu, R.-P., Yang, H., Xing, Y., Zhang, W.-P., Lambers, H., Li, L., Yu, R.-P., Yang, H., Xing, Y., Zhang, W.-P., Li, L., Lambers, H., 2022. Belowground processes and sustainability in agroecosystems with intercropping. Plant and Soil 476 (1), 263–288. https://doi.org/10.1007/S11104-022-05487-1.